


## Article

# Leader-follower formation tracking control of underactuated surface vehicles based on event-triggered control

Xiaoming Xia<sup>1</sup> \* , Zhaodi Yang<sup>1</sup>, Tianxiang Yang<sup>1</sup>

<sup>1</sup> School of Ocean Engineering, Jiangsu Ocean University, Lianyungang, China.

\* Correspondence: xia\_xm@126.com

**Abstract:** This paper investigates the leader–follower formation tracking control of underactuated surface vessels (USVs) with input saturation. Each vessel is subject to the uncertainties induced by model uncertainties and environmental disturbances. At first, an event-triggered extended state observer (ETESO) is used to recover the velocity, yaw rate and the uncertainties. Then, an estimator is used to estimate velocity of the leader. An event-triggered controller (ETC) is constructed based on the estimator, the observer and extra variables. Specifically, extra variables are used to solve the underactuated problem and input saturation. Stability analysis of control system is given to prove all signals are bounded. Simulations demonstrate that the ETESO can estimate accurately the uncertainties, the velocity and yaw rate; the ETC can largely reduce the action times of actuator.

**Keywords:** Leader–follower, event-triggered controller, underactuated surface vessels.

## 0. Introduction

In recent years, formation tracking control of underactuated surface vessels (USVs) has gained compelling interests, as they can be widely used in ocean engineering fields [1]. Compared with a single vessel, formation has many advantages. In the course of ocean exploration, the efficiency of a single vessel is low. Beyond that, formation can perform the complex tasks such as pursuing tasks that usually cannot accomplished by a single vessel. There are various formation control schemes include leader–follower approach [2][3], virtual structure [4], graph-based mechanism [5]. In particular, the leader-follower strategy is preferred in ocean engineering applications. The follower maintains a desired relative distance and angle with the leader, a reference trajectory can be defined by the leader. Therefore, the group behavior is directed by the leader, and the formation stability can be induced by the control law of single vessel.

There are two main challenges which are still worth mentioning. The first challenge is actuator saturation, it can severely degrade the closed-loop system performance [6]. In practice, each actuator of vessel can only provide a limited force or torque. To reduce the risk of actuator saturation and enhance system performance, some methods are proposed in recent years. To avoid a poor tracking performance in formation control, generalized saturation functions combined with formation tracking errors are employed to handle the input saturation problem [7]. To solve the input saturation and underactuated problems simultaneously, additional variables are induced to velocity errors in the body-fixed frame [8] [9]. Nonlinear saturation of actuator is approximated by a Gauss error function [10], such that anti-saturation controller can be designed. An auxiliary dynamic system is constructed to solve the input saturation problem [11]. The auxiliary dynamic system is designed as a second-order system, and it provides a conservative input signal. A first-order auxiliary system is designed [12], it is employed to deal with input saturation of rudder. However, the limited acting frequency of actuator is not considered in the above articles.

High-frequency action may lead not only to mechanical abrasion but also to a short service life [13]. Input saturation and actuator rate limits are considered in [14], and a nonlinear controller is designed based on dynamic surface control and a backstepping technology. [15] consider actuator saturation containing limited magnitude and rate, and design a sliding model controller. In [14] and [15], Zeno behavior is avoided because the

acting frequency of actuator is bounded. A controller combined with an event-triggered condition is proposed in [16], and the triggered condition is designed based on the flow time and error function. It still causes a large action times of actuator. [17] propose an event-triggered control law, and an event-triggered mechanism is used to reduce the execution frequency of actuators. The event-triggered mechanism is designed in the controller-to-actuator channel, the execution rate of the actuator are reduced.

**Table 1.** Notations and variables used in this paper.

|  |   |
|--|---|
| $\mathbb{R}^n$                                 | $n$ dimensional Euclidean Space   |
| $ \cdot $                                      | Absolute value of a variable  |
| $\lambda_{\min}(\cdot)$                        | Minimum eigenvalue of a matrix  |
| $\min\{\cdot\}$                                | Minimum value of a set  |
| $\inf\{\cdot\}$                                | Supremum of a set   |
| $(\cdot)^T$                                    | Transpose of a matrix   |
| $\ \cdot\ $                                    | Euclidean norm of a vector  |
| $\text{diag}\{\cdot\}$                         | Diagonal matrix   |
| $I_n$  | $n \times n$ dimensional identity matrix  |
| $0_n$  | $n \times n$ dimensional zero matrix.   |
| $(x_i, y_i), \psi_i, (x_j, y_j), \psi_j$       | Position and yaw of the $i$ th USV and the leader $j$                           |
| $u_i, v_i, r_i, u_j, v_j, r_j$                 | surge velocity, sway velocity and yaw rate of the $i$ th USV and the leader $j$ |
| $m_{i,11}, m_{i,22}, m_{i,33}$                 | inertia mass of the $i$ th USV  |
| $\sigma_{i,h}$                                 | Hydrodynamic damping parameters and disturbances                                |
| $\tau_i = [\tau_{i,u}, 0, \tau_{i,r}]$         | Input signals of the $i$ th USV   |
| $\eta_i, v_i$                                  | $\eta_i = [x_i, y_i, \psi_i]^T, v_i = [u_i, v_i, r_i]^T$                        |
| $\eta_j, v_j$                                  | $\eta_j = [x_j, y_j, \psi_j]^T, v_j = [u_j, v_j, r_j]^T$                        |
| $M_i$  | $M_i = \text{diag}\{m_{i,11}, m_{i,22}, m_{i,33}\}$                             |
| $R_i$  | Rotation matrices of the $i$ th USV   |
| $\tau_{ic} = [\tau_{i,uc}, 0, \tau_{i,rc}]^T$  | $\tau_{ic}$ calculated by the proposed controller                               |
| $\omega_i = [\omega_{i,u}, 0, \omega_{i,r}]^T$ | The mismatch function between input without saturation and with saturation      |
| $\rho_{ij}, \lambda_{ij}$                      | Relative distance and angle between the $i$ th USV and the leader $j$           |
| $\rho_{ij,d}, \lambda_{ij,d}$                  | Desired distance and angle  |
| $\hat{x}$                                      | Estimate of variable $x$  |
| $t_k$  | Previous event-triggering time instant  |
| $\xi_i$  | Transmitted signal between $\eta_i(t)$ and $\eta_i(t_k)$                        |
| $d(t)$   | Event-triggered mechanism   |
| $\tilde{x} = \hat{x} - x$                      | Estimation error of variable $x$  |
| $P_{ij} = [\rho_{ij,e}, \lambda_{ij,e}]^T$     | Formation tracking error vector   |
| $\hat{\Theta}_i$                               | Estimator used to estimate velocity of the leader                               |
| $l_{i,h}$                                      | Time constants of the first-order filters                                       |
| $\psi_{i,e}$                                   | Yaw tracking error  |
| $\beta_{i,h}$                                  | Virtual controls  |
| $\alpha_{i,h}$                                 | Auxiliary variables   |
| $\omega_{i,h}$                                 | Errors caused by the first order filter   |
| $\omega_{\tau u}, \omega_{\tau r}$             | Control laws at the kinetic level   |

The second significant challenge is the uncertainties. Because of the working condition of surface vessel, the uncertainties contain model uncertainties and environmental disturbances. In [18], the proposed controller is robust to the parameter uncertainties of the nonlinear terms and exogenous disturbances. Unknown plant parameters and environment disturbances are solved by using a parameter estimation and upper bound estimation in [19]. In [20], a robust adaptive control algorithm is proposed to solve uncertain parameters. Adaptive estimators are designed to estimate unknown time-varying functions of vessel model in [21]. Considering the leader-follower formation tracking problem, a neural network is used to approximate the uncertainties, and the uncertainties are compensated by on line learning [22]. A cooperative controller is proposed by using position-heading measurements only in [23], where an extended state observer (ESO) is constructed to provide the estimations of velocity, yaw rate and the uncertainties. However, the existing observers presented in [9], [11], [13], [17], [23], [24] rely on continuous sampling. In each

execution cycle signals are transmitted, which means that many network resources and calculation resources are consumed. To remove unnecessary calculation and communication, an event-triggered extended state observer (ETESO) is proposed in [25]. In [26], an ETESO is proposed for a class of nonlinear networked control systems, and the state estimation problem is solved. As for USVs, when their working mode is tracking control, in most cases, yaw angle is unchanging. In the common continuous observer, the signals have to be transmitted during each execution cycle, which will consume many network resources and calculation resources. Therefore, it is rewarding to design a leader-follower tracking controller with light transmission load and less action times of actuator.

Based on the above research background, this paper investigates leader-follower formation tracking control of USVs subject to input saturation, model uncertainties and environmental disturbances. Inspired by the works in [23] and [16], an improved output feedback controller is proposed. Firstly, an ETESO is used to recover the velocity data, model uncertainties and disturbances. In each execution cycle, an event-triggered strategy is monitored to determine whether or not to transmit the position and head informations to the observer. Sensor-to-observer communication costs are drastically reduced. Secondly, an estimator is employed to estimate velocity of the leader and reduce the amount of data exchanged in formation. Thirdly, auxiliary variables provide a solution of input saturation and underactuated problem. Then, an event-triggered controller (ETC) is designed based on the ETESO, the estimator and auxiliary variables. Finally, the stability of closed-loop system is proved. Simulations demonstrate the proposed control strategy.

Two salient features of the proposed control are summarized as follows. First, an estimator is employed to estimate the velocity of the leader, the embedded processor of each follower does reading computations only use the position and yaw of the leader, the transmission loads between formation are saved. Second, an event-triggered mechanism is designed in the controller-to-actuator channel, action times of actuator are reduced.

Compared with the existing related results, the novelty of this paper is summarized as follows. First, different from the existing formation control approaches [23] and [17], velocity of the leader is estimated by an estimator, which reduce the amount of data exchanged between USVs. Second, compared with the observer proposed in [23], the ETESO can reduce sensor-to-observer communication costs. Third, compared with the strategy proposed in [16], the proposed control law can largely reduce the action times of actuator.

The rest sections are organized as follows. A table of notations containing some used variables in the paper is presented. Section II describes the preliminaries and problem formulation. Section III describes observer design, Section IV gives controller design and stability analysis. Simulation results are presented in Section V. Section VI concludes this paper.

## 1. Problem formulation

A group of USVs consists  $N$  USVs, and the model of the  $i$ th USV is given as [27]

$$\dot{x}_i = u_i \cos(\psi_i) - v_i \sin(\psi_i), \quad (1)$$

$$\dot{y}_i = u_i \sin(\psi_i) + v_i \cos(\psi_i), \quad (2)$$

$$\dot{\psi}_i = r_i, \quad (3)$$

and

$$\dot{u}_i = \sigma_{i,1} + \frac{1}{m_{i,11}} \tau_{i,u}, \quad (4)$$

$$\dot{v}_i = \sigma_{i,2}, \quad (5)$$

$$\dot{r}_i = \sigma_{i,3} + \frac{1}{m_{i,33}} \tau_{i,r}, \quad (6)$$

where  $(x_i, y_i)^T \in \mathbb{R}^2$  is the position, and  $\psi_i$  is the yaw angle.  $u_i$  is the surge velocity,  $v_i$  is the sway velocity,  $r_i$  is the yaw rate.  $m_{i,11}$  and  $m_{i,33}$  denote the inertia mass. The uncertainties  $\sigma_{i,1}$ ,  $\sigma_{i,2}$  and  $\sigma_{i,3}$  contain Coriolis parameters, hydrodynamic damping parameters and time-varying disturbances.  $\tau_{i,u}$  and  $\tau_{i,r}$  are input signals.

To facilitate observer design and analysis, the  $i$ th USV model is written as

$$\dot{\eta}_i = R_i v_i \quad (7)$$

$$\dot{v}_i = M_i^{-1} \tau_i + \sigma_i, \quad (8)$$

where  $\eta_i = [x_i, y_i, \psi_i]^T$ ,  $v_i = [u_i, v_i, r_i]^T$ ,  $\tau_i = [\tau_{i,u}, 0, \tau_{i,r}]^T$ ,  $M_i = \text{diag}\{m_{i,11}, m_{i,22}, m_{i,33}\}$ ,  $m_{i,22}$  is the inertia mass.  $\sigma_i = [\sigma_{i,1}, \sigma_{i,2}, \sigma_{i,3}]^T$ ,

$$R_i = \begin{bmatrix} \cos(\psi_i) & -\sin(\psi_i) & 0 \\ \sin(\psi_i) & \cos(\psi_i) & 0 \\ 0 & 0 & 1 \end{bmatrix}.$$

The mismatch function between input without saturation and with saturation is described as  $\omega_i = [\omega_{i,u}, 0, \omega_{i,r}]^T = \tau_{ic} - \tau_i$ , where  $\tau_{ic} = [\tau_{i,uc}, 0, \tau_{i,rc}]^T$  with  $\tau_{i,uc}$  and  $\tau_{i,rc}$  are surge force and yaw moment calculated by the proposed controller, respectively.  $\tau_i = [\tau_{i,u}, 0, \tau_{i,r}]^T$ . Then, the saturated control is given by  $\tau_i = \tau_{ic} - \omega_i$ .

**Assumption 1:** The unknown function  $\sigma_i$  satisfies  $\dot{\sigma}_i \leq \sigma_i^*$  with  $\sigma_i^*$  is a positive constant.

$\sigma_i$  a vector containing velocity, Coriolis parameters, hydrodynamic damping parameters and time-varying disturbances. It is natural to assume that their derivatives are bounded. Control inputs to drive USVs are bounded, Assumption 1 is reasonable.

**Assumption 2:** Velocity of the  $i$ th USV is bounded, such that  $\|v_i\| \leq v_i^*$ ,  $v_i^*$  is a positive constant.

The control inputs to drive USVs are bounded, the energy of external disturbances is limited. Therefore, Assumption 2 is reasonable.

**Assumption 3:** The desired distance  $\rho_{ij,d}$  and angle  $\lambda_{ij,d}$  are bounded.

Assumption 3 means that the desired value is reasonable.

The following definitions are made.

The subscript  $j$  is the index of the leader  $j$ .  $\eta_j = [x_j, y_j, \psi_j]^T$  is used to denote the position and yaw of the leader  $j$ .  $v_j = [u_j, v_j, r_j]^T$  is the velocity and yaw rate of the leader  $j$ .

The relative distance  $\rho_{ij}$  and angle  $\lambda_{ij}$  between the  $i$ th USV and the leader  $j$  are expressed as

$$\rho_{ij} = \sqrt{(x_j - x_i)^2 + (y_j - y_i)^2}, \quad (9)$$

$$\lambda_{ij} = \text{atan2}(y_j - y_i, x_j - x_i). \quad (10)$$

The differential equations of  $\rho_{ij}$  and  $\lambda_{ij}$  are given by:

$$\begin{aligned} \dot{\rho}_{ij} &= \frac{(x_j - x_i)(\dot{x}_j - \dot{x}_i) + (y_j - y_i)(\dot{y}_j - \dot{y}_i)}{\sqrt{(x_j - x_i)^2 + (y_j - y_i)^2}} \\ &= \frac{(x_j - x_i)(\dot{x}_j - \dot{x}_i) + (y_j - y_i)(\dot{y}_j - \dot{y}_i)}{\rho_{ij}}, \end{aligned} \quad (11)$$

$$\dot{\lambda}_{ij} = \frac{1}{1 + \frac{(y_j - y_i)^2}{(x_j - x_i)^2}} \frac{(\dot{y}_j - \dot{y}_i)(x_j - x_i) - (\dot{x}_j - \dot{x}_i)(y_j - y_i)}{(x_j - x_i)^2}. \quad (12)$$

From  $x_j - x_i = \rho_{ij} \cos(\lambda_{ij})$  and  $y_j - y_i = \rho_{ij} \sin(\lambda_{ij})$ , then

$$\begin{aligned}\dot{\rho}_{ij} &= [u_j \cos(\psi_j) - v_j \sin(\psi_j) - u_i \cos(\psi_i) + v_i \sin(\psi_i)] \cos(\lambda_{ij}) \\ &\quad + [u_j \sin(\psi_j) + v_j \cos(\psi_j) - u_i \sin(\psi_i) + v_i \cos(\psi_i)] \sin(\lambda_{ij}) \\ &= -u_i \cos(\psi_i - \lambda_{ij}) + u_j \cos(\psi_j - \lambda_{ij}) \\ &\quad + v_i \sin(\psi_i - \lambda_{ij}) - v_j \sin(\psi_j - \lambda_{ij})\end{aligned}\quad (13)$$

$$\begin{aligned}\dot{\lambda}_{ij} &= \frac{(\dot{y}_j - \dot{y}_i)\rho_{ij} \cos(\lambda_{ij}) - (\dot{x}_j - \dot{x}_i)\rho_{ij} \sin(\lambda_{ij})}{\rho_{ij}^2} \\ &= \frac{1}{\rho_{ij}} \{-u_i \sin(\psi_i - \lambda_{ij}) + u_j \sin(\psi_j - \lambda_{ij}) \\ &\quad - v_i \cos(\psi_i - \lambda_{ij}) + v_j \cos(\psi_j - \lambda_{ij})\}.\end{aligned}\quad (14)$$

The control objective is to design an event-triggered control law for USVs to track the leader with desired distance  $\rho_{ij,d}$  and angle  $\lambda_{ij,d}$ .

**Remark 1.** In the controller design process, the  $i$ th USV track the  $j$ th USV by using the informations  $x_j$ ,  $y_j$  and  $\psi_j$ . It means that the communication costs between the multiple USVs are not saved.

## 2. Event-triggered extended state observer

An ETESO is developed for estimating the uncertainties containing model uncertainties and time-varying disturbances, and an event-triggered condition is employed to avoid unnecessary communications. Inspired by [25], an ETESO is designed as follow:

$$\dot{\hat{\eta}}_i(t) = -\frac{3}{\epsilon_i}(\hat{\eta}_i - \zeta_i) + R_i \hat{v}_i, \quad (15)$$

$$\dot{\hat{v}}_i(t) = -\frac{3}{\epsilon_i^2} R_i^T (\hat{\eta}_i - \zeta_i) + \hat{\sigma}_i + M_i^{-1} \tau_i, \quad (16)$$

$$\dot{\hat{\sigma}}_i(t) = -\frac{1}{\epsilon_i^3} R_i^T (\hat{\eta}_i - \zeta_i), \quad (17)$$

where  $\hat{\eta}_i = [\hat{x}_i, \hat{y}_i, \hat{\psi}_i]^T$ ,  $\hat{v}_i = [\hat{u}_i, \hat{v}_i, \hat{r}_i]^T$  and  $\hat{\sigma}_i = [\hat{\sigma}_{i,1}, \hat{\sigma}_{i,2}, \hat{\sigma}_{i,3}]^T$ .  $\hat{x}_i, \hat{y}_i, \hat{\psi}_i, \hat{u}_i, \hat{v}_i, \hat{r}_i, \hat{\sigma}_{i,1}, \hat{\sigma}_{i,2}$  and  $\hat{\sigma}_{i,3}$  are the estimates of  $x_i, y_i, \psi_i, u_i, v_i, r_i, \sigma_{i,1}, \sigma_{i,2}$  and  $\sigma_{i,3}$ , respectively.  $\epsilon_i$  is a positive constant and  $\zeta_i$  is the transmitted signal given by

$$\zeta_i(t) = \begin{cases} \eta_i(t_k), & \text{if } d(t) = 0 \\ \eta_i(t), & \text{otherwise.} \end{cases} \quad (18)$$

$t_k$  is the previous event-triggering time instant and  $d(t)$  is an event-triggered mechanism designed as

$$d(t) = \begin{cases} 0, & \text{if } \|q(t)\| < c_q \\ 1, & \text{otherwise.} \end{cases} \quad (19)$$

$c_q > 0$  is design threshold and

$$q(t) = [q_1, q_2, q_3]^T = [\eta_i(t_k) - \eta_i(t)] / \epsilon_i^2. \quad (20)$$

**Remark 2.** The continuous-time control scheme is emulated by computer with sampler and zero-order holder, and the control command is updated periodically. At each sampling instant,  $q(t)$  is monitored to determine whether or not to transmit the information  $\eta_i(t)$  to the observer. If  $\|q(t)\| \geq c_q$ , the event-triggering time instant  $t_k$  is updated to the current

time  $t$ , and  $\eta_i(t)$  is transmitted to the observer. Otherwise, only  $\eta_i(t_k)$  is available to the observer. The first event-triggering time is  $t_1 = 0$ .

To facilitate controller design and stability analysis, define  $\xi_i = [\xi_{i,1}, \xi_{i,2}, \xi_{i,3}]^T$ , (16) can be written as

$$\dot{\hat{u}}_i = \xi_{i,1} + \hat{\sigma}_{i,1} + \frac{\tau_{i,uc} - \omega_{i,u}}{m_{i,11}}, \quad (21)$$

$$\dot{\hat{\sigma}}_i = \xi_{i,2} + \hat{\sigma}_{i,2}, \quad (22)$$

$$\dot{\hat{r}}_i = \xi_{i,3} + \hat{\sigma}_{i,3} + \frac{\tau_{i,rc} - \omega_{i,r}}{m_{i,33}} \quad (23)$$

with

$$\xi_{i,1} = -\frac{3}{\epsilon_i^2} [\cos(\psi_i)(\hat{x}_i - \xi_{i,1}) + \sin(\psi_i)(\hat{y}_i - \xi_{i,2})], \quad (24)$$

$$\xi_{i,2} = -\frac{3}{\epsilon_i^2} [-\sin(\psi_i)(\hat{x}_i - \xi_{i,1}) + \cos(\psi_i)(\hat{y}_i - \xi_{i,2})], \quad (25)$$

$$\xi_{i,3} = -\frac{3}{\epsilon_i^2} (\hat{\psi}_i - \xi_{i,3}), \quad (26)$$

Define  $\tilde{x}_i = \hat{x}_i - x_i$ ,  $\tilde{y}_i = \hat{y}_i - y_i$ ,  $\tilde{\psi}_i = \hat{\psi}_i - \psi_i$ ,  $\tilde{u}_i = \hat{u}_i - u_i$ ,  $\tilde{\sigma}_i = \hat{\sigma}_i - \sigma_i$ ,  $\tilde{r}_i = \hat{r}_i - r_i$ ,

$$\tilde{\eta}_i = [\tilde{x}_i, \tilde{y}_i, \tilde{\psi}_i]^T, \quad e_{i,1}(t) = [e_{11}, e_{12}, e_{13}]^T = \frac{\tilde{\eta}_i(\epsilon_i t)}{\epsilon_i^2}, \quad (27)$$

$$\tilde{v}_i = [\tilde{u}_i, \tilde{\sigma}_i, \tilde{r}_i]^T, \quad e_{i,2}(t) = \frac{\tilde{v}_i(\epsilon_i t)}{\epsilon_i}, \quad (28)$$

$$\tilde{\sigma}_i = \hat{\sigma}_i - \sigma_i, \quad e_{i,3}(t) = \tilde{\sigma}_i(\epsilon_i t). \quad (29)$$

It follows that

$$\dot{e}_{i,1}(t) = -3e_{i,1}(t) - 3q(t) + R_i(\psi_i(t))e_{i,2}(t), \quad (30)$$

$$\dot{e}_{i,2}(t) = -3R_i^T(\psi_i(t))e_{i,1}(t) - 3R_i^T(\psi_i(t))q(t) + e_{i,3}(t), \quad (31)$$

$$\dot{e}_{i,3}(t) = -R_i^T(\psi_i(t))e_{i,1}(t) - R_i^T(\psi_i(t))q(t) - \epsilon_i \dot{\sigma}_i. \quad (32)$$

**Theorem 1.** Consider the USVs model (7) and (8), the ETESO (15), (16) and (17), and the event-triggering condition (19). If Assumptions 1 and 2 are satisfied, there exist  $\epsilon_i > 0$  and  $\iota > 0$  such that for any  $k > 0$ ,

$$\min\{t_{k+1} - t_k\} \geq \iota. \quad (33)$$

Proof. Along with (18) and (19), the event-triggering mechanism can be described as

$$\xi_i(t) = \begin{cases} \eta_i(t_k), & \text{if } \|\eta_i(t_k) - \eta_i(t)\| < c_q \epsilon_i^2 \\ \eta_i(t), & \text{otherwise.} \end{cases} \quad (34)$$

When  $t \in [t_k, t_{k+1})$ , the sample error  $\eta_i(t_k) - \eta_i(t)$  becomes

$$\begin{aligned} \|\eta_i(t_k) - \eta_i(t)\| &= \left\| \int_{t_k}^t \dot{\eta}_i(\iota) d\iota \right\| \\ &\leq \int_{t_k}^t \|R_i(\psi_i(\iota))v_i\| d\iota. \end{aligned} \quad (35)$$

Using Assumption 2, it obtains that

$$\|\eta_i(t_k) - \eta_i(t)\| \leq (t - t_k)v_i^*. \quad (36)$$

There exists  $\iota = \epsilon_i^2 c_q / v^*$  and  $\iota = t - t_k$ , such that  $\|\eta_i(t_k) - \eta_i(t)\| \leq c_q \epsilon_i^2$ . Notes that  $t \in [t_k, t_{k+1})$ , so it can draw a conclusion that  $\min\{t_{k+1} - t_k\} \geq \iota$ .

Theorem 1 shows that Zeno behavior can be avoided by using the proposed observer. Next, the error dynamics of the proposed ETESO are investigated.

To facilitate the stability analysis, define  $E_i(t) = [e_{i,1}(t)^T, e_{i,2}(t)^T, e_{i,3}(t)^T]^T \in \mathbb{R}^9$ , and the error dynamics (30)-(32) can be expressed as

$$\dot{E}_i(t) = A_i E_i(t) - B_i \epsilon_i \dot{\sigma}_i(t) - H_i D_i q(t), \quad (37)$$

$$A_i = \begin{bmatrix} -3I_3 & R_i(\psi_i(t)) & 0_3 \\ -3R_i^T(\psi_i(t)) & 0_3 & I_3 \\ -R_i^T(\psi_i(t)) & 0_3 & 0_3 \end{bmatrix}, \quad (38)$$

$$B_i = \begin{bmatrix} 0_3 \\ 0_3 \\ I_3 \end{bmatrix}, \quad (39)$$

$$D_i = \begin{bmatrix} 3_3 \\ 3_3 \\ I_3 \end{bmatrix}, \quad (40)$$

and  $H_i = \text{diag}\{I_3, R_i^T(\psi_i(t)), R_i^T(\psi_i(t))\}$ .

Using a transformation  $E_t(t) = T E_i(t)$  with  $T = \text{diag}\{R_i^T(\psi_i(t)), I_3, I_3\}$ , it follows that

$$\dot{E}_t(t) = A_0 E_t(t) + r_i S_T E_t(t) - B_i \epsilon_i \dot{\sigma}_i(t) - \bar{H}_i D_i q(t), \quad (41)$$

where  $\bar{H}_i = \text{diag}\{R^T(\psi_i(t)), R^T(\psi_i(t)), R^T(\psi_i(t))\}$ ,  $S_T = \text{diag}\{S^T, 0_3, 0_3\}$ , and

$$A_0 = \begin{bmatrix} -3I_3 & I_3 & 0_3 \\ -3I_3 & 0_3 & I_3 \\ -I_3 & 0_3 & 0_3 \end{bmatrix}, \quad (42)$$

$$S = \begin{bmatrix} 0 & -1 & 0 \\ 1 & 0 & 0 \\ 0 & 0 & 0 \end{bmatrix}. \quad (43)$$

**Theorem 3.** The observer error dynamics are bounded, if there exist a positive definite matrix  $P$  satisfying the inequalities used in stability analysis, the inequalities are defined as

$$A_0^T P + P A_0 + \varrho I_9 - \bar{r}_i (S_T^T P + P S_T) \leq 0, \quad (44)$$

$$A_0^T P + P A_0 + \varrho I_9 + \bar{r}_i (S_T^T P + P S_T) \leq 0, \quad (45)$$

where  $\varrho$  is a positive constant,  $\bar{r}_i$  is the upper bound of  $r_i$ .

**Proof.** Consider the Lyapunov function

$$V_o = \frac{1}{2} E_t(t)^T P E_t(t). \quad (46)$$





$z_i = [u_i, v_i]^T$ ,  $z_j = [u_j, v_j]^T$  and  $D_{ij,d} = [\dot{\rho}_{ij,d}, \dot{\lambda}_{ij,d}]^T$ .

Define  $f_i = [f_{i,1} \ f_{i,2}] = P_{ij}^T B_{ij} \Xi_{ij,1}$ ,  $\|f_i\| \leq f_i^*$ ,  $f_i^*$  is an unknown positive constant.

**Remark 3:** From the definition of  $\Xi_{ij,1}$ ,  $P_{ij}$  and  $B_{ij}$ , one notes that  $\|\Xi_{ij,1}\| = 1$ ,  $P_{ij}$  and  $B_{ij}$  are bounded, so  $\|f_i\| \leq f_i^*$  is reasonable.

Choosing  $\beta_i$  as a virtual controller,  $\beta_i$  is designed as:

$$\beta_i = \bar{\Xi}_{ij,1}^{-1} (B_{ij}^{-1} K_{i,1} P_{ij} + \hat{\Theta}_i - D_{ij,d}) + \bar{f}_{i,2} \quad (53)$$

where  $\bar{\Xi}_{ij,1}^{-1} = \Xi_{ij,1}^T (\Xi_{ij,1} \Xi_{ij,1}^T)^{-1}$ ,  $K_{i,1} \in \mathbb{R}^{2 \times 2}$  is a positive definite matrix,  $\bar{f}_{i,2} = [0, \tanh(f_{i,2}/\epsilon_f)]^T$ ,  $\epsilon_f > 0$  is a constant.  $\hat{\Theta}_i$  is the estimator of  $\Theta_i$ ,  $\Theta_i = \Xi_{ij,2} z_j$ , and it updates as

$$\dot{\hat{\Theta}}_i = -K_{\Theta} \hat{\Theta}_i - \bar{P}_{ij}, \quad (54)$$

$\bar{P}_{ij} = B_{ij} [\rho_{ij,e} \tanh(\rho_{ij,e}/\epsilon_\rho), \lambda_{ij,e} \tanh(\lambda_{ij,e}/\epsilon_\lambda)]^T$ ,  $K_{\Theta}$  is a positive definite matrix,  $\epsilon_\rho$  and  $\epsilon_\lambda$  are positive constants.

**Remark 4:** The adaptive term  $\hat{\Theta}_i$  is employed to reduce the volume of data on the formation communication [24], and estimate the information  $\Theta_i$ .  $\Theta_i$  can be estimated because  $\Xi_{ij,2} z_j \leq |z_j|$  and  $z_j$  is bounded. It makes sure that formation tracking control is achieved without velocity of the leader, the amount of data exchange between USVs can be reduced. Unlike the controller presented in [24], the proposed controller is designed without velocities of follower; the ETESO can reduce sensor-to-observer communication costs; the ETC can largely reduce the action times of actuator.

Step 2: Define a error as

$$\psi_{i,e} = \psi_i - \psi_{ij,a} \quad (55)$$

with

$$\psi_{ij,a} = [\arctan2(g_{ij,1}, g_{ij,2}) - \psi_j] \tanh(g_{ij,3}) + \psi_j, \quad (56)$$

where

$$g_{ij,1} = \rho_{ij} \sin(\lambda_{ij}) - \rho_{ij,d} \sin(\lambda_{ij,d}), \quad (57)$$

$$g_{ij,2} = \rho_{ij} \cos(\lambda_{ij}) - \rho_{ij,d} \cos(\lambda_{ij,d}), \quad (58)$$

$$g_{ij,3} = \{(\rho_{ij,d} - \rho_{ij})^2 + (\lambda_{ij,d} - \lambda_{ij})^2\} / \gamma_{ij}, \quad (59)$$

$\gamma_{ij}$  is a positive constant.

Using the the USV's dynamic, the time derivative of  $\psi_{i,e}$  is

$$\dot{\psi}_{i,e} = r_i - \dot{\psi}_{ij,a}. \quad (60)$$

The virtual control  $\beta_{i,3}$  is chosen as:

$$\beta_{i,3} = -k_{i,2} \psi_{i,e} + \dot{\psi}_{ij,a}, \quad (61)$$

where  $k_{i,2}$  is a positive constant.

Step 3: Define error functions as follow:

$$z_{i,e} = [u_{i,e}, v_{i,e}]^T = \hat{z}_i - \bar{\beta}_i - \gamma_1 \bar{\alpha}_i, \quad (62)$$

$$r_{i,e} = \hat{r}_i - \bar{\beta}_{i,3} - \gamma_1 \alpha_{i,3}, \quad (63)$$

$$\omega_i = \bar{\beta}_i - \beta_i, \quad (64)$$

$$\omega_{i,3} = \bar{\beta}_{i,3} - \beta_{i,3}, \quad (65)$$

where  $\hat{z}_i = [\hat{u}_i, \hat{v}_i]^T$ ,  $\bar{\beta}_i = [\bar{\beta}_{i,1}, \bar{\beta}_{i,2}]^T$ ,  $\gamma_1$  is a positive constant.  $\bar{\beta}_{i,h}$ ,  $h = 1, 2, 3$ , is derived from the first order filter  $l_{i,h}\dot{\bar{\beta}}_{i,h} + \bar{\beta}_{i,h} = \beta_{i,h}$ ,  $l_{i,h} > 0$  is a constant.  $\bar{\alpha}_i = [\alpha_{i,1}, \tanh(\alpha_{i,2})/\gamma_1]^T$ ,  $\alpha_{i,h}$ ,  $h = 1, 2, 3$ , is the auxiliary variable derived to deal with the underactuated problem and input saturation.  $\omega_i = [\omega_{i,1}, \omega_{i,2}]^T$ ,  $\omega_{i,h}$ ,  $h = 1, 2, 3$ , is the error caused by the first order filter.

The update laws of extra variables are given by

$$\dot{\alpha}_{i,1} = \frac{1}{\gamma_1}(-T_u \alpha_{i,1} - \frac{\omega_{i,u}}{m_{i,11}}), \quad (66)$$

$$\dot{\alpha}_{i,2} = \frac{1}{\cosh^2(\alpha_{i,2})}(\hat{\sigma}_{i,2} + k_{i,4}v_{i,e} - f_{i,2} - \dot{\bar{\beta}}_{i,2}), \quad (67)$$

$$\dot{\alpha}_{i,3} = \frac{1}{\gamma_1}(-T_r \alpha_{i,3} - \frac{\omega_{i,r}}{m_{i,33}}), \quad (68)$$

where  $T_u$ ,  $k_{i,4}$  and  $T_r$  are positive constants.

Step 4: A control law at the kinetic level is designed as

$$\omega_{\tau u}(t) = m_{i,11}(-k_{i,3}u_{i,e} + \dot{\bar{\beta}}_{i,1} - T_u \alpha_{i,1} + f_{i,1} - \hat{\sigma}_{i,1}), \quad (69)$$

$$\omega_{\tau r}(t) = m_{i,33}(-k_{i,5}r_{i,e} + \dot{\bar{\beta}}_{i,3} - T_r \alpha_{i,3} - \psi_{i,e} - \hat{\sigma}_{i,3}), \quad (70)$$

where  $k_{i,3}$  and  $k_{i,5}$  are positive constants.

**Remark 5:** In the common continuous control schemes, the controller design has already been completed in Step 4. Here, an event-triggered controller is designed and the event-triggered condition will be established in the following step. During the flow period between two successive triggering instants, zero-order holder is used to keep input signals unchanged. The key to a successful ETC design is to choose an appropriate event-triggered strategy. In [16], the triggered condition of time-varying threshold event-triggered controller (TTETC) is constructed based on flow time and Lyapunov function. Therefore, the action times of actuator is limited and Zeno behavior can be avoided. The signals calculated by controller should be closely related to the triggered condition, its size change determine whether or not to update the control inputs, and the change is used to design the proposed triggered condition. It is necessary to give the proof that Zeno behavior is avoided. The appropriate event-triggered strategy reduce the action times of actuator.

An event-triggered controller is chosen as

$$\begin{cases} \tau_{i,uc}(t) = \omega_{\tau u}(t_k^u), & \forall t \in [t_k^u, t_{k+1}^u) \\ \tau_{i,rc}(t) = \omega_{\tau r}(t_k^r), & \forall t \in [t_k^r, t_{k+1}^r) \end{cases} \quad (71)$$

with

$$\begin{cases} t_k^u = \inf\{t \in \mathbb{R} | |e_u(t)| \geq a_1\}, & t_1^u = 0 \\ t_k^r = \inf\{t \in \mathbb{R} | |e_r(t)| \geq a_2\}, & t_1^r = 0 \\ e_u = \omega_{\tau u} - \tau_{i,uc}, \quad e_r = \omega_{\tau r} - \tau_{i,rc}, \end{cases} \quad (72)$$

$a_1$  and  $a_2$  are positive constants.

The following theorem is given to point out the stability of overall closed-loop system.

**Theorem 3.** Consider the system consisting of the USV dynamics (7) and (8), the observer (15), (16) and (17), auxiliary variables (66), (67) and (68), the control law (71), with unknown environmental disturbances under Assumption 1-3. Then, the proposed control scheme guarantees: 1) All signals in the closed-loop system are bounded. 2) All USVs can track the leader with a bounded tracking error.

**Proof.** Choose a Lyapunov function candidate as follows :

$$V_1 = \frac{1}{2} P_{ij}^T P_{ij} + \frac{1}{2} \psi_{i,e}^2 + \frac{1}{2} u_{i,e}^2 + \frac{1}{2} v_{i,e}^2 + \frac{1}{2} r_{i,e}^2 + \frac{1}{2} \tilde{\Theta}_i^T \tilde{\Theta}_i + \frac{1}{2} \sum_{h=1}^3 \omega_{i,h}^2 + \frac{1}{2} \alpha_{i,1}^2 + \frac{1}{2} \alpha_{i,3}^2, \quad (73)$$

where  $\tilde{\Theta}_i = \hat{\Theta}_i - \Theta_i$ .

Along with (50) and (60), the time derivative of  $V_1$  is given

$$\begin{aligned} \dot{V}_1 = & P_{ij}^T B_i (-\Xi_{ij,1} z_i + \Xi_{ij,2} z_j - D_{ij,d}) + \psi_{i,e} (r_i - \dot{\psi}_{i,a}) \\ & + u_{i,e} (\dot{u}_i - \dot{\beta}_{i,1} - \gamma_1 \dot{\alpha}_{i,1}) + v_{i,e} (\dot{v}_i - \dot{\beta}_{i,2} - \dot{\alpha}_{i,2}) \\ & + r_{i,e} (\dot{r}_i - \dot{\beta}_{i,3} - \gamma_1 \dot{\alpha}_{i,3}) + \tilde{\Theta}_i^T \dot{\tilde{\Theta}}_i + \sum_{h=1}^3 \omega_{i,h} \dot{\omega}_{i,h} \\ & + \alpha_{i,1} \dot{\alpha}_{i,1} + \alpha_{i,3} \dot{\alpha}_{i,3}. \end{aligned} \quad (74)$$

By applying (21), (22), (23), (62) and (63) to (74), we obtain

$$\begin{aligned} \dot{V}_1 = & P_{ij}^T B_i [-\Xi_{ij,1} (z_{i,e} + \beta_i + \omega_i + \gamma_1 \bar{\alpha}_i - \bar{z}_i) + \Xi_{ij,2} z_j \\ & - D_{ij,d}] + \psi_{i,e} (r_{i,e} + \beta_{i,3} + \omega_{i,3} + \gamma_1 \alpha_{i,3} - \bar{r}_i \\ & - \dot{\psi}_{i,a}) + u_{i,e} (\zeta_{i,1} + \hat{\sigma}_{i,1} + \frac{\tau_{i,uc} - \omega_{i,u}}{m_{i,11}} - \dot{\beta}_{i,1} \\ & - \gamma_1 \dot{\alpha}_{i,1}) + v_{i,e} (\zeta_{i,2} + \hat{\sigma}_{i,2} - \dot{\beta}_{i,2} - \dot{\alpha}_{i,2}) \\ & + r_{i,e} (\zeta_{i,3} + \hat{\sigma}_{i,3} + \frac{\tau_{i,rc} - \omega_{i,r}}{m_{i,33}} - \dot{\beta}_{i,3} - \gamma_1 \dot{\alpha}_{i,3}) \\ & - \tilde{\Theta}_i^T K_{\Theta} \hat{\Theta}_i - \tilde{\Theta}_i^T \bar{P}_{ij} + \sum_{h=1}^3 \omega_{i,h} \dot{\omega}_{i,h} + \alpha_{i,1} \dot{\alpha}_{i,1} \\ & + \alpha_{i,3} \dot{\alpha}_{i,3}. \end{aligned} \quad (75)$$

Using (53), (54), (61), (66), (67) and (68) yields

$$\begin{aligned} \dot{V}_1 = & -P_{ij}^T K_{i,1} P_{ij} - k_{i,2} \psi_{i,e}^2 - P_{ij}^T B_{ij} \tilde{\Theta}_i \\ & - f_i (z_{i,e} + \omega_i + \gamma_1 \bar{\alpha}_i + \bar{f}_{i,2} - \bar{z}_i) \\ & + \psi_{i,e} (r_{i,e} + \omega_{i,3} + \gamma_1 \alpha_{i,3} - \bar{r}_i) \\ & + u_{i,e} (\zeta_{i,1} + \hat{\sigma}_{i,1} + \frac{\tau_{i,uc}}{m_{i,11}} - \dot{\beta}_{i,1} + T_u \alpha_{i,1}) \\ & + v_{i,e} (-k_{i,4} v_{i,e} + \zeta_{i,2} + f_{i,2}) \\ & + r_{i,e} (\zeta_{i,3} + \hat{\sigma}_{i,3} + \frac{\tau_{i,rc}}{m_{i,33}} - \dot{\beta}_{i,3} + T_r \alpha_{i,3}) \\ & - \tilde{\Theta}_i^T K_{\Theta} \hat{\Theta}_i - \tilde{\Theta}_i^T \bar{P}_{ij} - \sum_{h=1}^3 \omega_{i,h} (\frac{\omega_{i,h}}{l_{i,h}} + \dot{\beta}_{i,h}) \\ & - \bar{T}_u \alpha_{i,1}^2 - \alpha_{i,1} \bar{\omega}_{i,u} - \bar{T}_r \alpha_{i,3}^2 - \alpha_{i,3} \bar{\omega}_{i,r}, \end{aligned} \quad (76)$$

where  $\bar{T}_u = T_u / \gamma_1$ ,  $\bar{\omega}_{i,u} = \omega_{i,u} / m_{i,11}$ ,  $\bar{T}_r = T_r / \gamma_1$ ,  $\bar{\omega}_{i,r} = \omega_{i,r} / m_{i,33}$ .

According to (71) and (72), one has  $|\omega_{\tau u} - \tau_{i,uc}| \leq a_1$  and  $|\omega_{\tau r} - \tau_{i,rc}| \leq a_2$ . There exist time-varying functions  $\mu_1, \mu_2$  satisfying  $|\mu_1| \leq 1$  and  $|\mu_2| \leq 1$ . Then,  $\omega_{\tau u} = \tau_{i,uc} + \mu_1 a_1$  and  $\omega_{\tau r} = \tau_{i,rc} + \mu_2 a_2$ .

Notes that  $f_i z_{i,e} = f_{i,1} u_{i,e} + f_{i,2} v_{i,e}$  and

$$\begin{aligned} -P_{ij}^T B_{ij} \tilde{\Theta}_i - \tilde{\Theta}_i^T \bar{P}_{ij} &\leq |P_{ij}^T B_{ij} \tilde{\Theta}_i| - \tilde{\Theta}_i^T \bar{P}_{ij} \\ &\leq 0.2758\epsilon_p + 0.2758\epsilon_\lambda. \end{aligned} \quad (77)$$

Along with (69) and (70),  $\dot{V}_1$  becomes

$$\begin{aligned} \dot{V}_1 &\leq -P_{ij}^T K_{i,1} P_{ij} - k_{i,2} \psi_{i,e}^2 - k_{i,3} u_{i,e}^2 - k_{i,4} v_{i,e}^2 \\ &\quad - k_{i,5} r_{i,e}^2 - \bar{T}_u \alpha_{i,1}^2 - \bar{T}_r \alpha_{i,3}^2 - f_i (\omega_i + \gamma_1 \bar{\alpha}_i \\ &\quad + \bar{f}_{i,2} - \bar{z}_i) + \psi_{i,e} (\omega_{i,3} + \gamma_1 \alpha_{i,3} - \bar{r}_i) \\ &\quad + u_{i,e} (\zeta_{i,1} - \frac{\mu_1 a_1}{m_{i,11}}) + v_{i,e} \zeta_{i,2} + r_{i,e} (\zeta_{i,3} - \frac{\mu_2 a_2}{m_{i,33}}) \\ &\quad - \tilde{\Theta}_i^T K_\Theta \hat{\Theta}_i + 0.2758\epsilon_p + 0.2758\epsilon_\lambda \\ &\quad - \sum_{h=1}^3 \omega_{i,h} (\frac{\omega_{i,h}}{l_{i,h}} + \dot{\beta}_{i,h}) - \alpha_{i,1} \bar{\omega}_{i,u} - \alpha_{i,3} \bar{\omega}_{i,r}. \end{aligned} \quad (78)$$

According to Young's inequality,

$$\begin{aligned} -\tilde{\Theta}_i^T K_\Theta \hat{\Theta}_i &\leq -k_\Theta \tilde{\Theta}_i^T (\tilde{\Theta}_i + \Theta_i) \\ &\leq \frac{k_\Theta}{2} (-\tilde{\Theta}_i^T \tilde{\Theta}_i + \Theta_i^T \Theta_i) \end{aligned} \quad (79)$$

with  $k_\Theta = \lambda_{\min}(K_\Theta)$ .

$\dot{V}_1$  becomes

$$\begin{aligned} \dot{V}_1 &\leq -P_{ij}^T K_{i,1} P_{ij} - k_{i,2} \psi_{i,e}^2 - k_{i,3} u_{i,e}^2 - k_{i,4} v_{i,e}^2 \\ &\quad - k_{i,5} r_{i,e}^2 - \bar{T}_u \alpha_{i,1}^2 - \bar{T}_r \alpha_{i,3}^2 - \frac{k_\Theta}{2} \tilde{\Theta}_i^T \tilde{\Theta}_i \\ &\quad - f_i (\omega_i + \gamma_1 \bar{\alpha}_i + \bar{f}_{i,2} - \bar{z}_i) \\ &\quad + \psi_{i,e} (\omega_{i,3} + \gamma_1 \alpha_{i,3} - \bar{r}_i) + u_{i,e} (\zeta_{i,1} - \frac{\mu_1 a_1}{m_{i,11}}) \\ &\quad + v_{i,e} \zeta_{i,2} + r_{i,e} (\zeta_{i,3} - \frac{\mu_2 a_2}{m_{i,33}}) \\ &\quad - \sum_{h=1}^3 \omega_{i,h} (\frac{\omega_{i,h}}{l_{i,h}} + \dot{\beta}_{i,h}) - \alpha_{i,1} \bar{\omega}_{i,u} - \alpha_{i,3} \bar{\omega}_{i,r} \\ &\quad + \frac{k_\Theta}{2} \Theta_i^T \Theta_i + 0.2758\epsilon_p + 0.2758\epsilon_\lambda. \end{aligned} \quad (80)$$

According to [28] and Young's inequality,

$$\begin{aligned} -f_i (\gamma_1 \bar{\alpha}_{i,1} + \bar{f}_{i,2}) &= -\gamma_1 f_{i,1} \alpha_{i,1} - f_{i,2} \tanh(\alpha_{i,2}) \\ &\quad - \tanh(f_{i,2}/\epsilon_f) \\ &\leq \frac{\gamma_1^2}{2} f_{i,1}^2 + \frac{1}{2} \alpha_{i,1}^2 + 0.2785\epsilon_f. \end{aligned} \quad (81)$$

The following inequalities are used to stability analysis, which are represented as

$$\begin{aligned} f_i \bar{z}_i &= f_{i,1} \bar{u}_i + f_{i,2} \bar{v}_i \\ &\leq \frac{1}{2} (f_{i,1}^2 + f_{i,2}^2 + \bar{u}_i^2 + \bar{v}_i^2) \\ &\leq \frac{1}{2} (f_{i,1}^2 + f_{i,2}^2 + \epsilon_i^2 e_{11}^2 + \epsilon_i^2 e_{12}^2), \end{aligned} \quad (82)$$

$$\begin{aligned}\psi_{i,e}(\gamma_1\alpha_{i,3} - \tilde{r}_i) &\leq \frac{\gamma_1}{2}(\psi_{i,e}^2 + \alpha_{i,3}^2) + \frac{1}{2}\psi_{i,e}^2 + \frac{1}{2}\tilde{r}_i^2 \\ &\leq \frac{\gamma_1+1}{2}\psi_{i,e}^2 + \frac{\gamma_1}{2}\alpha_{i,3}^2 + \frac{1}{2}\epsilon_i^2 e_{13}^2,\end{aligned}\quad (83)$$

$$\begin{aligned}\zeta_{i,1} &\leq \frac{3}{\epsilon_i^2}(|\hat{x}_i - \zeta_{i,1}| + |\hat{y}_i - \zeta_{i,2}|) \\ &\leq 3(|e_{11}| + |q_1| + |e_{12}| + |q_2|),\end{aligned}\quad (84)$$

$$\begin{aligned}\zeta_{i,2} &\leq \frac{3}{\epsilon_i^2}(|\hat{x}_i - \zeta_{i,1}| + |\hat{y}_i - \zeta_{i,2}|) \\ &\leq 3(|e_{11}| + |q_1| + |e_{12}| + |q_2|),\end{aligned}\quad (85)$$

$$\zeta_{i,3} \leq \frac{3}{\epsilon_i^2}(|\hat{\psi}_i - \zeta_{i,3}|) \leq 3(|e_{13}| + |q_3|),\quad (86)$$

$$\begin{aligned}u_{i,e}(\zeta_{i,1} - \frac{\mu_1 a_1}{m_{i,11}}) &\leq u_{i,e}(\zeta_{i,1} + \bar{a}_1) \\ &\leq 3u_{i,e}(|e_{11}| + |q_1| + |e_{12}| + |q_2|) \\ &\quad + |u_{i,e}\bar{a}_1| \\ &\leq \frac{3}{2}(e_{11}^2 + q_1^2 + e_{12}^2 + q_2^2) + \frac{1}{2}\bar{a}_1 \\ &\quad + \frac{13}{2}u_{i,e}^2,\end{aligned}\quad (87)$$

$$\begin{aligned}v_{i,e}\zeta_{i,2} &\leq 3v_{i,e}(|e_{11}| + |q_1| + |e_{12}| + |q_2|) \\ &\leq \frac{3}{2}(e_{11}^2 + q_1^2 + e_{12}^2 + q_2^2) + 6v_{i,e}^2,\end{aligned}\quad (88)$$

$$\begin{aligned}r_{i,e}(\zeta_{i,3} - \frac{\mu_2 a_2}{m_{i,33}}) &\leq r_{i,e}(\zeta_{i,3} + \bar{a}_2) \\ &\leq 3r_{i,e}(|e_{13}| + |q_3|) + |r_{i,e}\bar{a}_2| \\ &\leq \frac{3}{2}(e_{13}^2 + q_3^2) + \frac{7}{2}r_{i,e}^2 + \frac{1}{2}\bar{a}_2^2,\end{aligned}\quad (89)$$

$$\alpha_{i,1}\bar{\omega}_{i,u} \leq \frac{1}{2}\alpha_{i,1}^2 + \frac{1}{2}\bar{\omega}_{i,u}^2,\quad (90)$$

$$\alpha_{i,3}\bar{\omega}_{i,r} \leq \frac{1}{2}\alpha_{i,3}^2 + \frac{1}{2}\bar{\omega}_{i,r}^2,\quad (91)$$

where  $\bar{a}_1 = a_1/m_{i,11}$ ,  $\bar{a}_2 = a_2/m_{i,33}$ .

Then, the following inequality can be obtained:

$$\begin{aligned}\dot{V}_1 \leq & -P_{ij}^T K_{i,1} P_{ij} - (k_{i,2} - \bar{\gamma}_1) \psi_{i,e}^2 - (k_{i,3} - \frac{13}{2}) u_{i,e}^2 \\ & - (k_{i,4} - 6) v_{i,e}^2 - (k_{i,5} - \frac{7}{2}) r_{i,e}^2 - \frac{k_\Theta}{2} \tilde{\Theta}_i^T \tilde{\Theta}_i \\ & - (\bar{T}_u - \frac{1}{2}) \alpha_{i,1}^2 - (\bar{T}_r - \bar{\gamma}_1) \alpha_{i,3}^2 - f_i \omega_i \\ & + \psi_{i,e} \omega_{i,3} - \sum_{h=1}^3 \omega_{i,h} (\frac{\omega_{i,h}}{l_{i,h}} + \dot{\beta}_{i,h}) + \frac{\epsilon_i^2 + 6}{2} e_{11}^2 \\ & + \frac{\epsilon_i^2 + 6}{2} e_{12}^2 + \frac{\epsilon_i^2 + 3}{2} e_{13}^2 + c_1,\end{aligned}\quad (92)$$

where  $\bar{\gamma}_1 = \frac{\gamma_1 + 1}{2}$ ,  $c_1 = \frac{k_\Theta}{2} \Theta_i^T \Theta_i + 0.2758 \epsilon_\rho + 0.2758 \epsilon_\lambda + \frac{\gamma_1^2}{2} f_{i,1}^2 + 0.2785 \epsilon_f + \frac{1}{2} (f_{i,1}^2 + f_{i,2}^2) + \frac{1}{2} \bar{\omega}_{i,u}^2 + \frac{1}{2} \bar{\omega}_{i,r}^2 + 3(q_1^2 + q_2^2 + \frac{1}{2} q_3^2) + \frac{1}{2} \bar{a}_1 + \frac{1}{2} \bar{a}_2$ .

Consider the total Lyapunov function as

$$V_2 = V_1 + V_o, \quad (93)$$

**Remark 5:** The Lyapunov function  $V_1$  include estimation errors  $e_{11}$ ,  $e_{12}$ ,  $e_{13}$ . We cannot conclude that  $\dot{V}_1 \leq -c_0 V_1 + c_3$ ,  $c_0$  and  $c_3$  are positive constants. The Lyapunov function  $V_2$  is constructed by inducing  $V_o$ . In the time derivative of  $V_2$ , the gain of estimation error is negative. We can conclude that  $\dot{V}_2 \leq -c_0 V_2 + c_3$ . Then, it is proved that all signals of the closed-loop system are bounded.

Along with (48) and (92), the time derivative of  $V_2$  is

$$\begin{aligned}\dot{V}_2 \leq & -P_{ij}^T K_{i,1} P_{ij} - (k_{i,2} - \bar{\gamma}_1) \psi_{i,e}^2 - (k_{i,3} - \frac{13}{2}) u_{i,e}^2 \\ & - (k_{i,4} - 6) v_{i,e}^2 - (k_{i,5} - \frac{7}{2}) r_{i,e}^2 - \frac{k_\Theta}{2} \tilde{\Theta}_i^T \tilde{\Theta}_i \\ & - (\bar{T}_u - \frac{1}{2}) \alpha_{i,1}^2 - (\bar{T}_r - \bar{\gamma}_1) \alpha_{i,3}^2 - f_i \omega_i \\ & + \psi_{i,e} \omega_{i,3} - \sum_{h=1}^3 \omega_{i,h} (\frac{\omega_{i,h}}{l_{i,h}} + \dot{\beta}_{i,h}) \\ & - c_2 \|E_t(t)\|^2 + c_1,\end{aligned}\quad (94)$$

where  $c_2 = \frac{q(1-c_{o1})}{2} - \frac{\epsilon_i^2 + 6}{2}$ .

Define  $\Omega_{i,1} = -f_{i,1} - \dot{\beta}_{i,1}$ ,  $\Omega_{i,2} = -f_{i,2} - \dot{\beta}_{i,2}$  and  $\Omega_{i,3} = \psi_{i,e} - \dot{\beta}_{i,3}$ . According to Young's inequality,  $\omega_{i,h} \Omega_{i,h} \leq \frac{1}{2q_c} \omega_{i,h}^2 \Omega_{i,h}^2 + \frac{q_c}{2}$ . Then,

$$\begin{aligned}\dot{V}_2 \leq & -P_{ij}^T K_{i,1} P_{ij} - (k_{i,2} - \bar{\gamma}_1) \psi_{i,e}^2 - (k_{i,3} - \frac{13}{2}) u_{i,e}^2 \\ & - (k_{i,4} - 6) v_{i,e}^2 - (k_{i,5} - \frac{7}{2}) r_{i,e}^2 - \frac{k_\Theta}{2} \tilde{\Theta}_i^T \tilde{\Theta}_i \\ & - (\bar{T}_u - \frac{1}{2}) \alpha_{i,1}^2 - (\bar{T}_r - \bar{\gamma}_1) \alpha_{i,3}^2 \\ & - \sum_{h=1}^3 (\frac{\omega_{i,h}^2}{l_{i,h}} - \frac{\omega_{i,h}^2 \Omega_{i,h}^2}{2q_c}) - c_2 \|E_t(t)\|^2 + c_3,\end{aligned}\quad (95)$$

where  $c_3 = c_1 + \frac{3}{2} q_c$ ,  $q_c$  is a positive constant.

Define  $|\Omega_{i,h}| \leq s_{i,h}$ ,  $s_{i,h}$ ,  $h = 1, 2, 3$  is a positive constant. Choosing  $\frac{1}{l_{i,h}^*} = s_{i,h}^2 / (2q_c) + l_{i,h}^*$  with  $l_{i,h}^* > 0$  is a constant. The follow can be attained:

$$\begin{aligned} \dot{V}_2 \leq & -P_{ij}^T K_{i,1} P_{ij} - (k_{i,2} - \bar{\gamma}_1) \psi_{i,e}^2 - (k_{i,3} - \frac{13}{2}) u_{i,e}^2 \\ & - (k_{i,4} - 6) v_{i,e}^2 - (k_{i,5} - \frac{7}{2}) r_{i,e}^2 - \frac{k_\Theta}{2} \tilde{\Theta}_i^T \tilde{\Theta}_i \\ & - (\bar{T}_u - \frac{1}{2}) \alpha_{i,1}^2 - (\bar{T}_r - \bar{\gamma}_1) \alpha_{i,3}^2 \\ & - \sum_{h=1}^3 l_{i,h}^* \omega_{i,h}^2 - \sum_{h=1}^3 (1 - \frac{\Omega_{i,h}^2}{s_{i,h}^2}) \frac{\omega_{i,h}^2 s_{i,h}^2}{2q_i} \\ & - c_2 \|E_t(t)\|^2 + c_3, \end{aligned} \quad (96)$$

Owing to  $|\Omega_{i,h}| \leq s_{i,h}$ , the inequality (96) becomes

$$\dot{V}_2 \leq -c_0 V_2 + c_3, \quad (97)$$

where  $c_0 = \min\{2\lambda_{\min}(K_{i,1}), 2(k_{i,2} - \bar{\gamma}_1), 2(k_{i,3} - \frac{13}{2}), 2(k_{i,4} - 6), 2(k_{i,5} - \frac{7}{2}), k_\Theta, 2(\bar{T}_u - \frac{1}{2}), 2(\bar{T}_r - \bar{\gamma}_1), 2l_{i,h}^*, 2c_2 / \lambda_{\max}(P)\}$ .

**Theorem 4.** The Zeno behavior can be avoided under the event-triggered mechanisms (71) and (72), and the implementation intervals  $t_{k+1}^u - t_k^u$  and  $t_{k+1}^r - t_k^r$  are lower bounded by a positive constant  $t^*$ .

**Proof.** According to (72), one has that

$$\begin{cases} \frac{d}{dt}|e_u| = \text{sign}(e_u)\dot{e}_u \leq |\dot{\omega}_{\tau u}|, & \forall t \in [t_k^u, t_{k+1}^u) \\ \frac{d}{dt}|e_r| = \text{sign}(e_r)\dot{e}_r \leq |\dot{\omega}_{\tau r}|, & \forall t \in [t_k^r, t_{k+1}^r) \end{cases} \quad (98)$$

The time derivatives of  $\omega_{\tau u}$  and  $\omega_{\tau r}$  are given

$$\dot{\omega}_{\tau u}(t) = m_{i,11}(-k_{i,3}\dot{u}_{i,e} + \ddot{\beta}_{i,1} - T_u\dot{\alpha}_{i,1} + \dot{f}_{i,1} - \dot{\hat{\sigma}}_{i,1}), \quad (99)$$

$$\dot{\omega}_{\tau r}(t) = m_{i,33}(-k_{i,5}\dot{r}_{i,e} + \ddot{\beta}_{i,3} - T_r\dot{\alpha}_{i,3} - \dot{\psi}_{i,e} - \dot{\hat{\sigma}}_{i,3}). \quad (100)$$

Theorem 3 shows that all signals in the closed-loop system are bounded. Then,  $\dot{u}_{i,e}$ ,  $\dot{r}_{i,e}$ ,  $\ddot{\beta}_{i,1}$ ,  $\ddot{\beta}_{i,3}$ ,  $\dot{\alpha}_{i,1}$ ,  $\dot{\alpha}_{i,3}$  and  $\dot{\psi}_{i,e}$  are bounded. According to the design of ETESO,  $\dot{\hat{\sigma}}_{i,1}$  and  $\dot{\hat{\sigma}}_{i,3}$  are bounded.  $\dot{f}_{i,1}$  is bounded because  $\|f_i\| \leq f_i^*$ . Therefore, there are positive constants  $k_u$  and  $k_r$  satisfying  $|\dot{\omega}_{\tau u}| \leq k_u$  and  $|\dot{\omega}_{\tau r}| \leq k_r$ . Since

$$\begin{cases} e_u(t_k^u) = 0, & \lim_{t \rightarrow t_{k+1}^u} |e_u(t)| = a_1 \\ e_r(t_k^r) = 0, & \lim_{t \rightarrow t_{k+1}^r} |e_r(t)| = a_2 \end{cases} \quad (101)$$

there exists the lower bound of implementation interval  $t^*$  and  $t^* \geq \min\{a_1/k_u, a_2/k_r\}$ . Hence, no Zeno phenomenon will occur by using the proposed control law.

#### 4. Simulation Results

In this section, simulation results are proposed to prove the proposed event-triggered control method, and the ship parameters are chosen from [29]. Four USVs are driven to track a leader at a desired distance and angle with the proposed control law in (69)-(72). The total duration of the simulation runs is 120s, the sampling time  $t_s$  for each time point is 0.01s. The initial positions of followers are chosen as:  $\eta_1(0) = [-2 \text{ m}, -5 \text{ m}, 0 \text{ rad}]^T$ ,  $\eta_2(0) = [-2 \text{ m}, 5 \text{ m}, 0 \text{ rad}]^T$ ,  $\eta_3(0) = [-4 \text{ m}, -8 \text{ m}, 0 \text{ rad}]^T$ ,  $\eta_4(0) = [-4 \text{ m}, 8 \text{ m}, 0 \text{ rad}]^T$ . The trajectory of leader is generated by:  $u_j = 0.2 \text{ m/s}$ ,  $v_j = 0 \text{ m/s}$  and  $r_j = 0 \text{ rad/s}$  for  $0 \leq t < 40 \text{ s}$ ,  $u_j = 0.2 \text{ m/s}$ ,  $v_j = 0 \text{ m/s}$  and  $r_j = 0.1 \text{ rad/s}$  for  $40 \leq t < 60 \text{ s}$ ,  $u_j = 0.2 \text{ m/s}$ ,  $v_j = 0 \text{ m/s}$  and  $r_j = -0.1 \text{ rad/s}$  for  $60 \leq t < 80 \text{ s}$ ,  $u_j = 0.2 \text{ m/s}$ ,  $v_j = 0 \text{ m/s}$  and  $r_j = 0 \text{ rad/s}$  for  $80 \leq t < 120 \text{ s}$ ,  $\eta_j(0) = [0 \text{ m}, 0 \text{ m}, 0 \text{ rad}]^T$ . The desired distance

and relative angle are given by  $\rho_{1j,d} = 3$  m,  $\lambda_{1j,d} = 1$  rad,  $\rho_{2j,d} = 3$  m,  $\lambda_{2j,d} = -1$  rad,  $\rho_{3j,d} = 6$  m,  $\lambda_{3j,d} = 1$  rad,  $\rho_{4j,d} = 6$  m,  $\lambda_{4j,d} = -1$  rad.

The parameters of ETESO are chosen as:  $\epsilon_i = 0.4$ ,  $c_q = 0.1$ . The parameters of the proposed control law are chosen as  $\epsilon_f = 0.1$ ,  $K_{\Theta} = \text{diag}\{5, 5\}$ ,  $\gamma_{ij} = 0.001$ ,  $K_{i,1} = \text{diag}\{5, 5\}$ ,  $k_{i,2} = 5$ ,  $k_{i,3} = 10$ ,  $k_{i,4} = 10$ ,  $k_{i,5} = 10$ ,  $\gamma_1 = 5$ ,  $T_u = 10$ ,  $T_r = 16$ ,  $l_{i,h} = 0.1$ ,  $h = 1, 2, 3$ . The parameters of trigger condition are  $a_1 = a_2 = 0.2$ .

**Remark 6:** According to inequality (97), we should keep  $c_0$  as large as possible and  $c_3$  as small as possible. The close-loop system can converge quickly with small errors. However,  $c_3$  include the mismatch variables between input without saturation and with saturation  $\bar{\omega}_{i,u}$  and  $\bar{\omega}_{i,r}$ . Large gain factors  $K_{i,1}$ ,  $k_{i,2}$ ,  $k_{i,3}$ ,  $k_{i,4}$  and  $k_{i,5}$  corresponds to large mismatch variables. Therefore, we make gain factor as small as possible without violating the constraint  $c_0 > 0$ .  $\gamma_1$ ,  $T_u$  and  $T_r$  define the convergence rate of auxiliary variables, and they satisfy the inequalities  $T_u/\gamma_1 - 1/2 > 0$  and  $T_r/\gamma_1 - (1 + \gamma_1)/2 > 0$ .  $l_{i,h}$  determines the tracking speed of first order filter, which is related to sampling time of simulation. And too large value will make an unstable system, too small value will make a poor tracking performance. As a rule of thumb, the general recommended value of  $l_{i,h}$  is between  $t_s$  and  $10t_s$ . The parameters  $a_1$  and  $a_2$  define trigger condition of the proposed controller, larger  $a_1$  and  $a_2$  mean lower update frequency of input signals and a poor system performance. To find a balance between update frequency and system performance,  $a_1$  and  $a_2$  are defined as  $a_1 = a_2 = 0.2$ .  $\epsilon_i$  define the estimation speed of ETESO,  $c_q$  is the threshold of trigger condition of ETESO, and the process of parameter selection is similar to parameter selection in  $a_1$  and  $a_2$ .

For surface vessels, the effect of gravity can be neglected because gravity acting on USVs equals buoyancy acting on USVs. The USVs are subject to model uncertainties and environmental disturbances. Model uncertainties are induced by model errors and unknown system parameters. Therefore, only Centrifugal terms, damping parameters and environmental disturbances are considered. In this paper, the uncertainties  $\sigma_{i,1}$ ,  $\sigma_{i,2}$  and  $\sigma_{i,3}$  are assumed to be unknown. Environmental disturbances contain wind, wave and current. The impacts on USVs of wind can be ignored due to small windward area. Therefore, environmental disturbances are designed as the sum of some sinusoidal signals, which are chosen as  $[0.18 - 0.18 \cos(0.01t) \cos(0.015t), 0.6 + 0.18 \sin(0.21t) \cos(0.2t), 0.6 - 0.18 \sin(0.2t) \cos(0.23t)]^T$ .

Simulation results are shown in Figs. 3-8. Fig. 3 shows formation pattern shaped by the five vessels, and all followers can successfully track the leader. Fig. 4 shows that the formation tracking errors approach zero regardless of model uncertainties and environmental disturbances. Fig. 5 shows the input signals of four USVs. In the first 24s, since initial formation tracking errors are large, saturated control inputs suffer from sudden jumps. During 25s-40s, formation tracking errors approach zero, input signals convergences gradually. At 40s, 60s and 80s, the sudden changes of the control forces are caused by sudden change of the leader velocity.

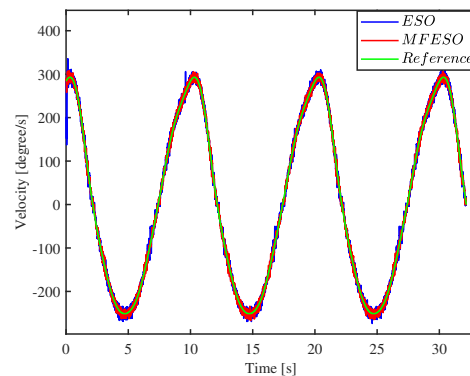


**Figure 2.** Formation pattern with four followers and a leader.



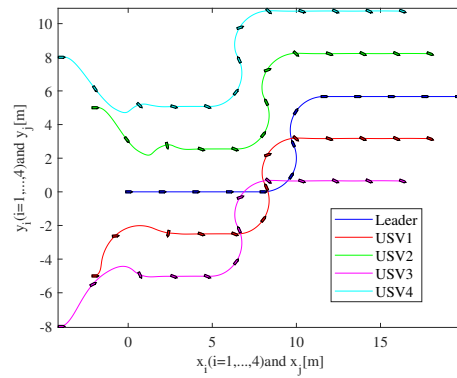


**Figure 3.** Formation pattern with four followers and a leader.

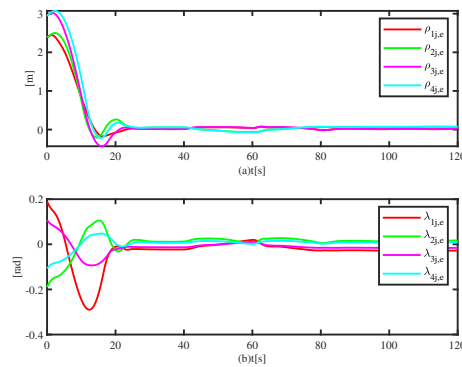


**Figure 4.** Tracking errors with perturbations effect.

The comparison of simulation results are shown in Fig. 6-8, simulations are conducted using the TTETC proposed in [16] and the ETC proposed in this paper. The two controllers have same control parameters, different parameters of trigger condition.

The TTETC is designed as follows:

$$\begin{cases} \tau_{i,uc}(t) = \omega_{\tau u}(t_k^u), & \forall t \in [t_k^u, t_{k+1}^u) \\ \tau_{i,rc}(t) = \omega_{\tau r}(t_k^r), & \forall t \in [t_k^r, t_{k+1}^r) \end{cases} \quad (102)$$

with

$$\begin{cases} t_k^u = \inf\{t \in \mathbb{R} | t > t_{k-1}^u \wedge e_u > \sigma V_2 \wedge V_2 > \mu\}, & t_1^u = 0 \\ t_k^r = \inf\{t \in \mathbb{R} | t > t_{k-1}^r \wedge e_r > (1 - \sigma)V_2 \wedge V_2 > \mu\}, & t_1^r = 0 \\ e_u = \omega_{\tau u} - \tau_{i,uc}, & e_r = \omega_{\tau r} - \tau_{i,rc}, \end{cases} \quad (103)$$

$\mu = 0.02, \sigma = 0.5$ .

Fig. 6 depicts formation pattern shaped by the  $i$ th USV and the leader. The different controllers are applied to the system with and without perturbations, respectively. It reveals that the follower is able to track the leader successfully under four different conditions. Fig. 7 depicts the distance and angle tracking errors under four different conditions, and it shows the errors converge to a small neighborhood of the origin. Compared with the system with perturbations, the system without perturbations has faster convergent rate. In the system with perturbations, some control energy is used to reject disturbances including model uncertainties and environmental disturbances. Then, the energy that make the system convergent is reduced. Under the same condition, stability errors and convergence rates of TTETC and ETC are nearly the same. The two controllers have same structure but

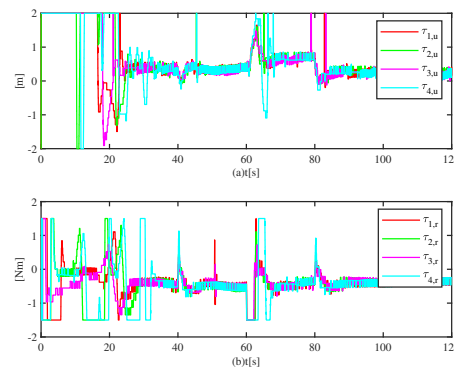


**Figure 5.** Input signals of four USVs.

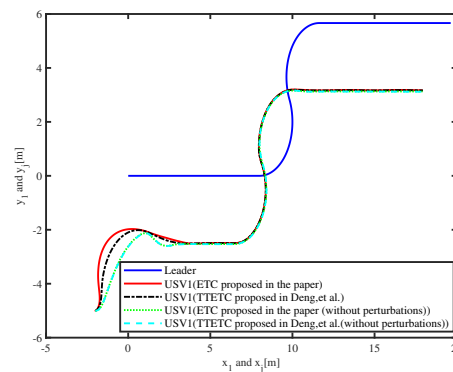
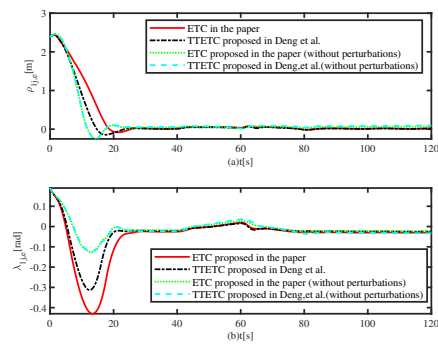


**Figure 6.** Leader-follower formation tracking control under four conditions.

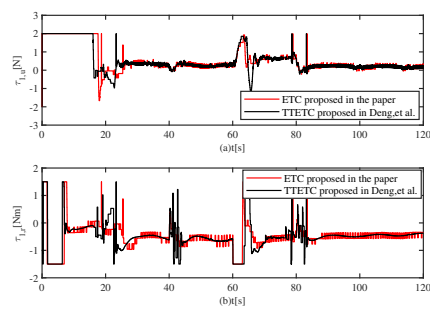
different event-triggered strategy. Therefore, they have same convergent rate but different action times of actuator. Fig. 8 depicts the control signals generated by the two different controllers. By the effect of the proposed controller, the input signals are shaking in low frequencies, but the amplitudes are higher. At the beginning, due to large initial formation tracking error, the input signals are saturated. The input signals converge along with the convergence of formation tracking error. At 40s, 60s and 80s, the input signals are shaking due to change of the leader velocity. Fig. 9 shows the control inputs at the first 20 seconds, and the update frequencies of control inputs are different due to different triggering strategies.

Fig. 10 is the event-based release instants and release intervals of input signals under the proposed controller. As shown in Table 2, compared with TTETC, the proposed ETC largely reduce the action times of actuator. The triggering condition of TTETC is designed based on the Lyapunov function  $V_2$ . In order to assure the performance of control systems, the threshold is set to a smaller value. The threshold of ETC is set to 0.2, the action times of actuator can be largely reduced.

The ESO is proposed in [23]. Fig. 11 shows the estimated velocities and real velocities, illustrating that velocity estimate of ETESO is as good as that of ESO. Fig. 12 shows the uncertainties are effectively approximated by ESO and ETESO. Comparing to ESO, ETESO simultaneously get large steady error and large jitter. Fig. 13 shows the event-based release instants and release intervals of ETESO, a local enlarged drawing is also given. During 40 – 45 s, the maximum release interval is 0.08, and the minimum release interval is 0.01. During 0 – 120 s, most of release intervals are greater than 0.04. Therefore, some communication times are saved. Table 3 shows communication times of two observers. A counter is added in simulation. When the event condition is met, the counter begin to



**Figure 7.** Tracking errors under different controllers.



**Figure 8.** Control inputs with perturbations effect.

count. After the application completes, the counter shows the total number of times the event has occurred. Communication times can be attained by multiplying the total number of times by the sampling time. Compared with ESO, the ETESO can reduce communication costs and communication time. The ETESO is applied to reduce communication costs in the cost of losing estimation accuracy.

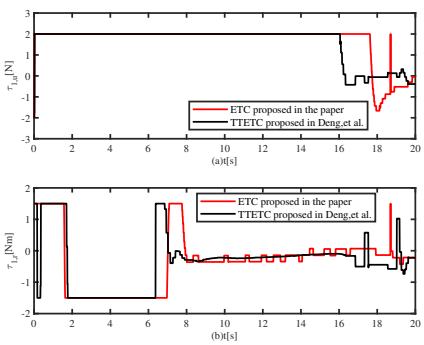


Figure 9. Local enlarged diagram around of Fig. 8.

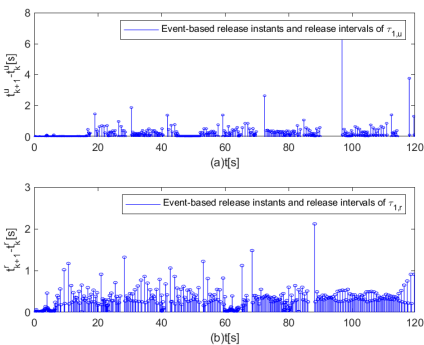


Figure 10. The event-based release instants and release intervals of input signals.

Table 2. The comparisons of ETC and TTETC

| Performance parameter                                    | ETC      | TTETC    |
|--|----------|----------|
| Convergent time  | 24.25s   | 24.26s   |
| Convergent time (without perturbations)                  | 24.21s   | 24.22s   |
| stability error $\rho_{1j,e}$                            | 0.01m    | 0.01m    |
| Stability error $\rho_{1j,e}$ (without perturbations)    | 0.01m    | 0.01m    |
| Stability error $\lambda_{1j,e}$                         | -0.02rad | -0.02rad |
| Stability error $\lambda_{1j,e}$ (without perturbations) | -0.01rad | -0.01rad |
| Action times of $\tau_{1,uc}$                            | 1321     | 2226     |
| Action times of $\tau_{1,uc}$ (without perturbations)    | 1210     | 2064     |
| Action times of $\tau_{1,rc}$                            | 702      | 2226     |
| Action times of $\tau_{1,rc}$ (without perturbations)    | 504      | 2064     |

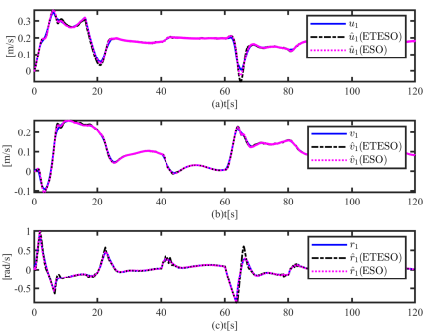


Figure 11. Comparisons of estimation performance.

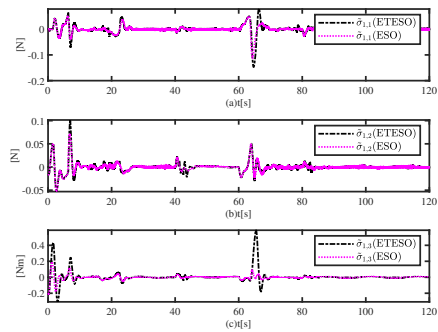


Figure 12. The approximation errors under different observers.

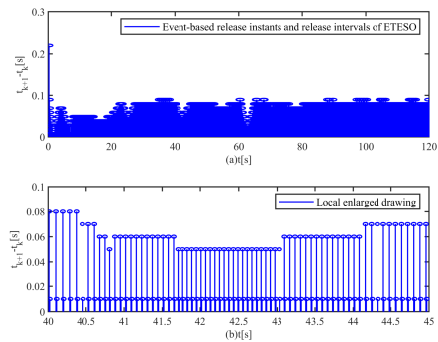


Figure 13. The triggering instants for the ETESO and its local enlarged drawing.

Table 3. The comparisons of communication time.

| Serial number | Variable | Time (s) |
|---------------|----------|----------|
| (1)           | ETESO    | 31.84    |
| (2)           | ESO      | 120      |

## 5. Conclusion

This article suggests an output feedback controller for surface vessel with model uncertainties, unknown environmental disturbances, and input constraints. Static obstacles and unknown non-cooperative ships are also considered. An ESO is given, unknown model dynamics and velocity are simultaneously estimated. The controller is designed based on the ADS and MAPFs. Finally, the mathematic analysis is given to proved that all error signals of the system are bounded. Simulation experiments affirm the tracking performance of the proposed controller.

**Author Contributions:** Conceptualization, methodology, software, writing—review and editing, Xiaoming Xia; validation, Zhaodi Yang; writing—review and editing, Tianxiang Yang.

**Funding:** This work is supported by the Funded by the 7th Generation Ultra Deep Water Drilling unit Innovation Project.

**Institutional Review Board Statement:** This article does not contain any studies with human or animal subjects.

**Data Availability Statement:** The data of this paper is unavailable.

**Conflicts of Interest:** The authors declare no conflict of interest.

## References

- Peng, Z.; Wang, J.; Wang, D.; Han, Q.L. An Overview of Recent Advances in Coordinated Control of Multiple Autonomous Surface Vehicles. *IEEE Transactions on Industrial Informatics* **2021**, *17*, 732–745. <https://doi.org/10.1109/TII.2020.3004343>.
- Cui, R.; Ge, S.; How, B.; Choo, Y. Leader–Follower Formation Control of Underactuated Autonomous Underwater Vehicles. *Ocean Engineering* **2010**, *37*, 1491–1502. <https://doi.org/10.1016/j.oceaneng.2010.07.006>.
- Xia, G.; Xia, X.; Zhao, B.; Sun, C.; Sun, X. A Solution to Leader Following of Underactuated Surface Vessels with Actuator Magnitude and Rate Limits. *International Journal of Adaptive Control and Signal Processing* **2021**, *35*, 1860–1878. <https://doi.org/10.1002/acs.3294>.
- Beard, R.; Lawton, J.; Hadaegh, F. A Coordination Architecture for Spacecraft Formation Control. *IEEE Transactions on Control Systems Technology* **2001**, *9*, 777–790. <https://doi.org/10.1109/87.960341>.
- Park, B.S.; Yoo, S.J. An Error Transformation Approach for Connectivity-Preserving and Collision-Avoiding Formation Tracking of Networked Uncertain Underactuated Surface Vessels. *IEEE Transactions on Cybernetics* **2019**, *49*, 2955–2966. <https://doi.org/10.1109/TCYB.2018.2834919>.
- Chen, M.; Ge, S.S.; How, B.V.E.; Choo, Y.S. Robust Adaptive Position Mooring Control for Marine Vessels. *IEEE Transactions on Control Systems Technology* **2013**, *21*, 395–409. <https://doi.org/10.1109/TCST.2012.2183676>.
- Shojaei, K. Leader–Follower Formation Control of Underactuated Autonomous Marine Surface Vehicles with Limited Torque. *Ocean Engineering* **2015**, *105*, 196–205. <https://doi.org/10.1016/j.oceaneng.2015.06.026>.
- Park, B.S.; Kwon, J.W.; Kim, H. Neural Network-Based Output Feedback Control for Reference Tracking of Underactuated Surface Vessels. *Automatica* **2017**, *77*, 353–359. <https://doi.org/10.1016/j.automatica.2016.11.024>.
- Xia, G.; Xia, X.; Zhao, B.; Sun, C.; Sun, X. Distributed Tracking Control for Connectivity-Preserving and Collision-Avoiding Formation Tracking of Underactuated Surface Vessels with Input Saturation. *Applied Sciences* **2020**, *10*, 3372. <https://doi.org/10.3390/app10103372>.
- Deng, Y.; Zhang, X.; Im, N.; Zhang, G.; Zhang, Q. Adaptive Fuzzy Tracking Control for Underactuated Surface Vessels with Unmodeled Dynamics and Input Saturation. *ISA Transactions* **2020**, *103*, 52–62. <https://doi.org/10.1016/j.isatra.2020.04.010>.
- Xia, G.; Xia, X.; Sun, X. Formation Control with Collision Avoidance for Underactuated Surface Vehicles. *Asian Journal of Control* **2021**, *24*, 2244–2257. <https://doi.org/10.1002/asjc.2620>.
- Liu, C.; Chen, C.L.P.; Zou, Z.; Li, T. Adaptive NN-DSC Control Design for Path Following of Underactuated Surface Vessels with Input Saturation. *Neurocomputing* **2017**, *267*, 466–474. <https://doi.org/10.1016/j.neucom.2017.06.042>.
- Xia, G.; Xia, X.; Bo, Z.; Sun, X.; Sun, C. Event-Triggered Controller Design for Autopilot with Input Saturation. *Mathematical Problems in Engineering* **2020**, *2020*, e5362895. <https://doi.org/10.1155/2020/5362895>.
- von Ellenrieder, K.D. Dynamic Surface Control of Trajectory Tracking Marine Vehicles with Actuator Magnitude and Rate Limits. *Automatica* **2019**, *105*, 433–442. <https://doi.org/10.1016/j.automatica.2019.04.018>.
- Wang, S.; Gao, Y.; Liu, J.; Wu, L. Saturated Sliding Mode Control with Limited Magnitude and Rate. *IET Control Theory & Applications* **2018**, *12*, 1075–1085. <https://doi.org/10.1049/iet-cta.2017.1081>.
- Deng, Y.; Zhang, X.; Im, N.; Zhang, G.; Zhang, Q. Event-Triggered Robust Fuzzy Path Following Control for Underactuated Ships with Input Saturation. *Ocean Engineering* **2019**, *186*, 106122. <https://doi.org/10.1016/j.oceaneng.2019.106122>.
- Peng, Z.; Jiang, Y.; Wang, J. Event-Triggered Dynamic Surface Control of an Underactuated Autonomous Surface Vehicle for Target Enclosing. *IEEE Transactions on Industrial Electronics* **2021**, *68*, 3402–3412. <https://doi.org/10.1109/TIE.2020.2978713>.

18. Ahmad, I.; Ouannas, A.; Shafiq, M.; Pham, V.T.; Baleanu, D. Finite-Time Stabilization of a Perturbed Chaotic Finance Model. *Journal of Advanced Research* **2021**, *32*, 1–14. <https://doi.org/10.1016/j.jare.2021.06.013>.
19. Sun, Z.; Zhang, G.; Lu, Y.; Zhang, W. Leader-Follower Formation Control of Underactuated Surface Vehicles Based on Sliding Mode Control and Parameter Estimation. *ISA Transactions* **2018**, *72*, 15–24. <https://doi.org/10.1016/j.isatra.2017.11.008>.
20. Ahmad, I.; Shafiq, M. Oscillation Free Robust Adaptive Synchronization of Chaotic Systems with Parametric Uncertainties. *Transactions of the Institute of Measurement and Control* **2020**, *42*, 1977–1996. <https://doi.org/10.1177/0142331220903668>.
21. Jin, X. Fault Tolerant Finite-Time Leader–Follower Formation Control for Autonomous Surface Vessels with LOS Range and Angle Constraints. *Automatica* **2016**, *68*, 228–236. <https://doi.org/10.1016/j.automatica.2016.01.064>.
22. Peng, Z.h.; Wang, D.; Lan, W.y.; Sun, G. Robust Leader-Follower Formation Tracking Control of Multiple Underactuated Surface Vessels. *China Ocean Engineering* **2012**, *26*, 521–534. <https://doi.org/10.1007/s13344-012-0039-8>.
23. Peng, Z.; Wang, D.; Li, T.; Han, M. Output-Feedback Cooperative Formation Maneuvering of Autonomous Surface Vehicles With Connectivity Preservation and Collision Avoidance. *IEEE Transactions on Cybernetics* **2020**, *50*, 2527–2535. <https://doi.org/10.1109/TCYB.2019.2914717>.
24. Lu, Y.; Zhang, G.; Qiao, L.; Zhang, W. Adaptive Output-Feedback Formation Control for Underactuated Surface Vessels. *International Journal of Control* **2020**, *93*, 400–409. <https://doi.org/10.1080/00207179.2018.1471221>.
25. Liu, L.; Zhang, W.; Wang, D.; Peng, Z. Event-Triggered Extended State Observers Design for Dynamic Positioning Vessels Subject to Unknown Sea Loads. *Ocean Engineering* **2020**, *209*, 107242. <https://doi.org/10.1016/j.oceaneng.2020.107242>.
26. Yu, Y.; Yuan, Y.; Yang, H.; Liu, H. A Novel Event-Triggered Extended State Observer for Networked Control Systems Subjected to External Disturbances. *International Journal of Robust and Nonlinear Control* **2019**, *29*, 2026–2040. <https://doi.org/10.1002/rnc.4476>.
27. Do, K.; Jiang, Z.; Pan, J. Underactuated Ship Global Tracking under Relaxed Conditions. *IEEE Transactions on Automatic Control* **2002**, *47*, 1529–1536. <https://doi.org/10.1109/TAC.2002.802755>.
28. Polycarpou, M. Stable Adaptive Neural Control Scheme for Nonlinear Systems. *IEEE Transactions on Automatic Control* **1996**, *41*, 447–451. <https://doi.org/10.1109/9.486648>.
29. Skjetne, R.; Fossen, T.I.; Kokotović, P.V. Adaptive Maneuvering, with Experiments, for a Model Ship in a Marine Control Laboratory. *Automatica* **2005**, *41*, 289–298. <https://doi.org/10.1016/j.automatica.2004.10.006>.